

EUROPEAN ORGANIZATION FOR NUCLEAR RESEARCH

LHWG Note 2001-04  
ALEPH 2001-057 CONF 2001-037  
DELPHI 2001-114 CONF 537  
L3 Note 2700  
OPAL Technical Note TN699  
October 24, 2018

# Searches for the Neutral Higgs Bosons of the MSSM: Preliminary Combined Results Using LEP Data Collected at Energies up to 209 GeV

The ALEPH, DELPHI, L3 and OPAL Collaborations,  
and the LEP Higgs Working Group

## Abstract

In the year 2000 the four LEP experiments collected data at centre-of-mass energies between 200 and 209 GeV, integrating approximately  $870 \text{ pb}^{-1}$  of luminosity, with about  $510 \text{ pb}^{-1}$  above 206 GeV. The LEP working group for Higgs boson searches has combined these data with data sets collected previously at lower energies. In representative scans of the parameters of the Minimal Supersymmetric Standard Model (MSSM), the mass limits  $m_{h^0} > 91.0 \text{ GeV}/c^2$  and  $m_{A^0} > 91.9 \text{ GeV}/c^2$  are obtained for the light CP-even and the CP-odd neutral Higgs boson, respectively. For a top quark mass less than or equal to  $174.3 \text{ GeV}/c^2$ , assuming that the stop quark mixing is maximal, and choosing conservative values for other SUSY parameters affecting the Higgs sector, the range  $0.5 < \tan \beta < 2.4$  is excluded. Additionally, the results of flavour-independent searches for hadronically decaying Higgs bosons are included, allowing exclusion of MSSM models with suppressed decays of the Higgs bosons to pairs of b quarks.

**All results quoted in this note are preliminary.**

# 1 Introduction

This note describes a combination of preliminary results of searches for the neutral Higgs bosons of the Minimal Supersymmetric Standard Model (MSSM) by the four LEP collaborations, ALEPH, DELPHI, L3 and OPAL. The results are based on data collected at  $\sqrt{s} \approx 200 - 209$  GeV, the highest  $e^+e^-$  collision energies attained at LEP, and are combined with data collected earlier at lower centre-of-mass energies.

The MSSM predicts the existence of two complex scalar field doublets, with a total of eight degrees of freedom. As in the Standard Model (SM), three degrees of freedom appear as the longitudinal polarization states of the gauge bosons  $W^+$ ,  $W^-$  and  $Z^0$ . The remaining five degrees of freedom are manifested in five physical scalar Higgs states. In this note, the Higgs sector of the MSSM is assumed to conserve CP. Under this assumption, the physical Higgs bosons are the CP-even  $h^0$  and  $H^0$ , the CP-odd  $A^0$ , and the charged bosons  $H^+$  and  $H^-$ . The quartic self-coupling of the Higgs fields are determined by the gauge couplings, which limits the mass of the lighter of the two CP-even Higgs bosons to be less than the mass of the  $Z^0$  at tree level. Radiative corrections, particularly from loops containing the top quark, allow the lightest Higgs boson mass to range up to approximately  $135 \text{ GeV}/c^2$ , which is its maximal value [1–8] for all choices of parameters in the MSSM models within the constrained framework considered in this note (see Section 3.1). This constraint on the mass of the  $h^0$  suggests that the  $h^0$  may be light enough to be produced at LEP. Searches are performed for the possible final states containing Higgs bosons and they are combined among the four collaborations in order to place the tightest constraints on the possible values of the parameters of the MSSM Higgs sector.

In the MSSM, the Higgs-strahlung process  $e^+e^- \rightarrow h^0 Z^0$  proceeds as in the Standard Model, but its rate is suppressed by the factor  $\sin^2(\beta - \alpha)$ , where  $\tan \beta$  is the ratio of the vacuum expectation values of the two field doublets, and  $\alpha$  is the mixing angle in the neutral CP-even Higgs boson sector. The WW- and ZZ-fusion processes of the SM also proceed with a rate suppressed by the same factor relative to the SM rate. Heavy-Higgs-strahlung,  $e^+e^- \rightarrow H^0 Z^0$ , occurs if it is kinematically possible, and has the SM production cross-section suppressed by the factor  $\cos^2(\beta - \alpha)$ . In some cases  $e^+e^- \rightarrow H^0 Z^0$  can have a higher cross-section than  $e^+e^- \rightarrow h^0 Z^0$ . The process  $e^+e^- \rightarrow h^0 A^0$  also occurs when kinematically allowed, and its production cross-section is proportional to  $\cos^2(\beta - \alpha)$ . Dedicated analyses are used to search for this final state.

The Higgs boson sector of the MSSM corresponds to a Type II two-Higgs-doublet model, in that the couplings of the Higgs fields to the fermions are constrained such that at tree level one Higgs field couples to the up-type fermions and the other to the down-type fermions and the charged leptons. This is arranged in order to avoid loop anomalies, to prevent flavour-changing neutral currents, and to give mass to the up-type and down-type fermions. This structure also implies that the decay branching ratios of the Higgs bosons to fermions depend not only on the masses, but also on the values of  $\alpha$  and  $\beta$ . At tree level, the coupling of the  $h^0$  to  $b\bar{b}$  is proportional to  $-\sin \alpha / \cos \beta$ , the coupling of the  $h^0$  to  $c\bar{c}$  is proportional to  $\cos \alpha / \sin \beta$ , the coupling of the  $A^0$  to  $b\bar{b}$  is proportional to  $\tan \beta$ , and the coupling of the  $A^0$  to  $c\bar{c}$  is proportional to  $\cot \beta$ . Over much of the parameter space considered, the  $h^0$  and the  $A^0$  decay predominantly into  $b\bar{b}$  and  $\tau^+\tau^-$  pairs, although for various choices of parameters, the decays  $h^0 \rightarrow A^0 A^0$ ,  $h^0 \rightarrow c\bar{c}$ ,  $h^0 \rightarrow gg$  and  $h^0 \rightarrow W^+W^-$  can become important.

The searches that are combined in this note are the searches for the  $e^+e^- \rightarrow h^0 Z^0$  (and WW- and ZZ-fusion) processes which are used in the Standard Model interpretations

presented separately by the four collaborations in [9–12], combined with the searches for the  $e^+e^- \rightarrow h^0 A^0$  process described in [13–16]. In addition, for models in which the decay branching ratios of the Higgs bosons to  $b\bar{b}$  and  $\tau^+\tau^-$  are suppressed, the flavour-independent results are used [16–21]. In all combinations, a full specification of the production cross-sections at all relevant centre-of-mass energies and all decay branching ratios are incorporated into the calculations of the expected signal rates. The searches combined are sensitive predominantly to the  $b\bar{b}$  and  $\tau^+\tau^-$  decays of the  $h^0$  and the  $A^0$ . A number of the searches mentioned above also have estimated efficiencies for the decays  $h^0 \rightarrow c\bar{c}$ ,  $gg$ ,  $W^+W^-$ ,  $A^0 A^0$  (with specified decays of the  $A^0$ , usually only to  $b\bar{b}$ ), etc. The signal estimations for these searches also include the contributions from these sources. The Higgs boson masses, cross-sections and decay branching ratios are computed using HZHA03 [22], modified to use either the FeynHiggs calculations [7, 23, 24] or SUBHPOLE2 [5].

Each experiment has generated Monte Carlo simulations of the signal processes and the SM background processes, typically at centre-of-mass energies of 200, 202, 204, 206, 208 and 210 GeV. The rates and distributions for energies in between the Monte Carlo points are interpolated.

The statistical procedure adopted for the combination of the data and the definitions of the test statistic  $-2 \ln Q$  and the confidence levels  $CL_s$ ,  $CL_{s+b}$  and  $CL_b$ , are described in [25]. The main sources of systematic uncertainty in the estimations of the accepted signal and background rates are incorporated using an extension of the method of Cousins and Highland [26], where the correlations arising from shared error sources between analyses conducted at different energies, and between similar analyses conducted by the separate collaborations, are taken into account.

Searches for charged Higgs bosons are presented separately in [27].

## 2 Searches for $e^+e^- \rightarrow h^0 A^0$

The analyses of the full data sample for the  $h^0 Z^0$  processes are documented in [9–12]. This section describes only the results of searches for  $e^+e^- \rightarrow h^0 A^0$ . In the MSSM,  $\cos^2(\beta - \alpha)$  is significantly different from zero only when  $\tan \beta$  is large ( $> 8$ ) and  $m_{A^0}$  is less than the maximum allowed  $m_{h^0}$  (depending on the parameters of the scenario). The models with  $\cos^2(\beta - \alpha)$  significantly different from zero have  $m_{h^0} \approx m_{A^0}$ . The  $b\bar{b}$  and  $\tau^+\tau^-$  decays of the  $h^0$  and  $A^0$  are dominant for such models, and the searches concentrate on these decays only. The numbers of selected events, the expected signal for  $m_{h^0}=90 \text{ GeV}/c^2$  and  $m_{A^0}=90 \text{ GeV}/c^2$ , and the estimated background from SM processes are shown in Table 1, separately for each experiment. Also listed are the integrated luminosities reported by the experiments for the data taken in the year 2000. Due to the  $\beta^3$  kinematical factor dependence of the production cross-section for  $e^+e^- \rightarrow h^0 A^0$ , the expected limits on the  $m_{h^0}=m_{A^0}$  diagonal are  $10 \text{ GeV}/c^2$  below the average energy of the LEP2 data in 2000, and so the precise distribution of the beam energy is of less importance to the sensitivity of the  $h^0 A^0$  searches than it is to the  $h^0 Z^0$  searches.

	ALEPH	DELPHI	L3	OPAL
<b><math>h^0 A^0 \rightarrow b\bar{b}b\bar{b}</math> channel</b>				
Integrated Luminosity ( $\text{pb}^{-1}$ )	217	224	217	208
Data	10	5	13	11
Total Background	5.5	6.5	9.4	10.3
Four-Fermion Bkg.	4.2	4.4	7.3	6.9
$q\bar{q}$ Background	1.4	2.1	2.1	3.4
Efficiency				
$m_{h^0} = m_{A^0} = 90 \text{ GeV}/c^2$	47%	47%	42%	48%
Expected signal				
$m_{h^0} = m_{A^0} = 90 \text{ GeV}/c^2$	3.5	3.6	3.2	3.4
<b><math>h^0 A^0 \rightarrow b\bar{b}\tau^+\tau^-</math> channel</b>				
Integrated Luminosity ( $\text{pb}^{-1}$ )	217	224	217	205
Data	3	5	2	5
Total Background	3.0	6.0	3.0	4.5
Four-Fermion Bkg.	2.8	5.6	2.8	4.1
$q\bar{q}$ Background	0.2	0.4	0.4	0.4
Efficiency				
$m_{h^0} = m_{A^0} = 90 \text{ GeV}/c^2$	41%	25%	33%	43%
Expected signal				
$m_{h^0} = m_{A^0} = 90 \text{ GeV}/c^2$	0.6	0.4	0.4	0.6
Limit obs (exp.med) for $m_{h^0}$ ( $\text{GeV}/c^2$ )	89.6 (91.7)	89.7 (88.8)	83.2 (88.1)	79.3 (85.1)
Limit obs (exp.med) for $m_{A^0}$ ( $\text{GeV}/c^2$ )	90.0 (92.1)	90.7 (89.7)	83.9 (88.3)	80.6 (86.9)

Table 1: The results in the  $h^0 A^0$  channels for each experiment for the data taken in 2000. Listed are the individual signal efficiencies, the expected signal counts, the total backgrounds, the backgrounds broken down into  $q\bar{q}$  and four-fermion sources and the observed data counts, for each experiment's  $h^0 A^0 \rightarrow b\bar{b}b\bar{b}$  and  $h^0 A^0 \rightarrow b\bar{b}\tau^+\tau^-$  channel separately. The “tight selection” is shown for DELPHI's  $h^0 A^0 \rightarrow b\bar{b}b\bar{b}$  channel for easier comparison with the other experiments. The L3 results are also shown with tighter selections than are used in the combinations for easier comparison. The signal efficiencies and rates are given for  $m_{h^0} = m_{A^0} = 90 \text{ GeV}/c^2$ , with  $\tan\beta \sim 20$ . Also listed are the observed and median expected lower bounds on  $m_{h^0}$  and  $m_{A^0}$ , taking the lower values of the limits obtained in the no-mixing and  $m_{h^0}$ -max scenarios. These scenarios are discussed in Section 3.

### 3 Limits in the MSSM Parameter Space

The  $h^0Z^0$  and  $h^0A^0$  searches at LEP in the year 2000 are combined with previous LEP Higgs searches presented in [28] and references therein, conducted at centre-of-mass energies between  $\sim 88$  GeV and 202 GeV.

#### 3.1 Benchmark Scenarios

We test for the presence of an MSSM Higgs boson signal using a constrained model with seven parameters,  $M_{\text{SUSY}}$ ,  $M_2$ ,  $\mu$ ,  $A$ ,  $\tan\beta$ ,  $m_{A^0}$  and  $m_{\tilde{g}}$ . All of the soft SUSY-breaking parameters in the sfermion sector are set to  $M_{\text{SUSY}}$  at the electroweak scale.  $M_2$  is the SU(2) gaugino mass parameter at the electroweak scale, and  $M_1$  is derived from  $M_2$  using the GUT relation  $M_1 = M_2(5 \sin^2\theta_W/3 \cos^2\theta_W)$ , where  $\theta_W$  is the weak mixing angle<sup>1</sup>. The supersymmetric Higgs boson mass parameter is denoted  $\mu$ , and  $\tan\beta$  is the ratio of the vacuum expectation values of the two Higgs field doublets. The parameter  $A$  is the common trilinear Higgs-squark coupling parameter, assumed to be the same for up-type squarks and for down-type squarks. The largest contributions to  $m_{h^0}$  from radiative corrections arise from stop loops, with much smaller contributions from sbottom loops. The gluino mass  $m_{\tilde{g}}$  affects loop corrections from both stops and sbottoms. The mass of the top quark is assumed to be 174.3 GeV/ $c^2$ , the current average [29] of the TeVatron measurements.

Three benchmark scenarios are considered [30]. The first (“no-mixing” scenario) assumes that there is no mixing between the scalar partners of the left-handed and the right-handed top quarks, with the following values and ranges for the parameters:  $M_{\text{SUSY}} = 1$  TeV/ $c^2$ ,  $M_2 = 200$  GeV/ $c^2$ ,  $\mu = -200$  GeV/ $c^2$ ,  $X_t(\equiv A - \mu \cot\beta) = 0$ ,  $0.4 < \tan\beta < 50$  and  $4$  GeV/ $c^2 < m_{A^0} < 1$  TeV/ $c^2$ . The gluino mass  $m_{\tilde{g}}$  is set to 800 GeV/ $c^2$ ; it has little effect on the phenomenology of this scenario. Most of the experimental Monte Carlo samples assume that the  $h^0$  and  $A^0$  have decay widths which are small compared to the resolutions of the reconstructed masses; only DELPHI has performed tests in which the  $h^0$  and  $A^0$  widths are significant [14]. The assumption that the decay widths can be neglected is only valid for  $\tan\beta < 30$  in this scenario, and hence higher values of  $\tan\beta$  are not considered.

The second scenario (“ $m_{h^0}$ -max”) is designed to yield the maximal value of  $m_{h^0}$  in the model. The  $m_{h^0}$ -max scenario corresponds to the most conservative range of excluded  $\tan\beta$  values for fixed values of the mass of the top quark and  $M_{\text{SUSY}}$ . The dependence of the limit on  $\tan\beta$  on the top quark mass is given in Section 3.2.1. The values of the parameters in the  $m_{h^0}$ -max scenario are fixed at the same values used in the no-mixing scenario, except for the stop mixing parameter  $X_t = 2M_{\text{SUSY}}$ , using the conventions of the two-loop diagrammatic calculation of [7,23]. Only values of  $\tan\beta$  below 30 are considered in this model also in order to satisfy the assumptions made on the decay widths.

The third scenario (“large  $\mu$ ” scenario) is a scan with parameters chosen to be  $M_{\text{SUSY}} = 400$  GeV/ $c^2$ ,  $\mu = 1$  TeV/ $c^2$ ,  $M_2 = 400$  GeV/ $c^2$ ,  $m_{\tilde{g}} = 200$  GeV/ $c^2$ ,  $4 \leq m_{A^0} \leq 400$  GeV/ $c^2$ ,  $X_t = -300$  GeV/ $c^2$ . This third scenario is designed to illustrate choices of MSSM parameters for which the Higgs boson  $h^0$  does not decay into pairs of b quarks due to large corrections from SUSY loop processes. This situation occurs mostly at  $\tan\beta > 20$  and for  $120 < m_{A^0} < 220$  GeV/ $c^2$ . The dominant decay modes of the  $h^0$

---

<sup>1</sup> $M_3$ ,  $M_2$  and  $M_1$  are the mass parameters associated with the SU(3), SU(2) and U(1) subgroups of the Standard Model. The relevance of  $M_3$  only enters via loop corrections sensitive to the gluino mass.

for these models are to  $c\bar{c}$ ,  $gg$ ,  $W^+W^-$  and  $\tau^+\tau^-$ . For many of these models, the decay  $h^0 \rightarrow \tau^+\tau^-$  is also suppressed, providing an additional experimental challenge. In this scenario, for all choices of  $m_{A^0}$  and  $\tan\beta$ , at least one Higgs boson signal with a large production cross-section is within the kinematic reach of LEP2. The maximum value of  $m_{h^0}$  in this scenario is slightly less than  $108 \text{ GeV}/c^2$ . For some choices of  $m_{A^0}$  and  $\tan\beta$ , the  $h^0 Z^0$  cross-section is suppressed by a small value of  $\sin^2(\beta - \alpha)$ , and  $e^+e^- \rightarrow h^0 A^0$  is not within the kinematic reach of LEP2. For these models, however, the heavy Higgs  $H^0$  has a mass less than  $109 \text{ GeV}/c^2$ , and may be produced in Higgs-strahlung. The value of  $\text{Br}(H^0 \rightarrow b\bar{b})$  may be suppressed, however. For all choices of parameters within the recommended ranges in the large  $\mu$  scenario, the decay widths of the  $h^0$  and the  $A^0$  remain small when compared with the resolutions on the reconstructed masses. For this reason, the full recommended range of  $\tan\beta$  up to 50 is considered in this scenario, in contrast to the first two scenarios.

For the no-mixing and  $m_{h^0}$ -max scenarios, the two-loop diagrammatic approach of [7, 23] is used to compute the relations between the SUSY parameters,  $m_{h^0}$ ,  $m_{A^0}$ ,  $m_{H^\pm}$ ,  $\tan\beta$ , and the production cross-sections and decay branching ratios. For the large  $\mu$  scenario, the one-loop renormalization-group improved calculation of [5, 31, 32] is used. These two calculations give consistent results [32, 33], although small differences still exist. For example, in the  $m_{h^0}$ -max scenario, the diagrammatic approach gives a more conservative upper edge of the excluded region of  $\tan\beta$ , while one-loop renormalization-group improved approach gives a slightly more conservative lower edge. The value of  $m_{h^0}$  predicted by FeynHiggs is uncertain at the 2–3  $\text{GeV}/c^2$  level, due to uncalculated subleading and higher-order corrections. A recent calculation is available [8] which incorporates subleading two-loop top-Yukawa terms not yet included in FeynHiggs, although its applicability is limited to situations with  $m_{A^0} \gg m_{Z^0}$ . The differences with the FeynHiggs calculation fall within the 2–3  $\text{GeV}/c^2$  uncertainty, and are smaller than those induced by the current uncertainty in the top quark mass. The effect of the uncertain top quark mass on the  $\tan\beta$  limit is given below.

## 3.2 Results

The calculations of the confidence levels are performed for the three benchmark scenarios separately, and the results are shown in this section. The  $m_{h^0}$ -max and no-mixing scenarios are described together in Section 3.2.1, while the large  $\mu$  scenario is described separately in Section 3.2.2 because of qualitative differences in the features of these scenarios.

### 3.2.1 The $m_{h^0}$ -max and No-Mixing Scenarios

Figure 1 shows the  $1 - \text{CL}_b$  significance contours as functions of  $h^0$  mass and  $A^0$  mass for the  $m_{h^0}$ -max scenario. An excess is seen at  $(m_{h^0}, m_{A^0}) \sim (83, 83) \text{ GeV}/c^2$ , with a significance level slightly in excess of  $2\sigma$ . This is due to candidates in the OPAL 189  $\text{GeV}$   $\tau^+\tau^-b\bar{b}$  channel [34] which have not been confirmed by later running or in other experiments; the significance has gradually decreased as additional luminosity has been accumulated. Another excess is seen near  $(m_{h^0}, m_{A^0}) \sim (93, 93) \text{ GeV}/c^2$ , due to candidates in the OPAL four-jet channel in the data taken in 2000 [16], which also does not appear in other samples. The current 95% CL exclusion limits from LEP (shown also in the same figure) rules out the possibility of a signal with  $(m_{h^0}, m_{A^0}) \sim (83, 83) \text{ GeV}/c^2$

within the MSSM models considered, but is not strong enough to exclude the  $(m_{h^0}, m_{A^0}) \sim (93, 93)$  GeV/ $c^2$  hypothesis. There are two excesses in the  $h^0 Z^0$  searches which appear as vertical bands in Figure 1, at  $m_{h^0} \approx 97$  GeV/ $c^2$ , and at  $m_{h^0} \approx 115$  GeV/ $c^2$ . The excess at  $m_{h^0} = 97$  GeV/ $c^2$  is present in the 189 GeV data collected in 1998 [35], but does not appear in the 192–202 GeV data collected in 1999 [28]. Its significance is only slightly over  $2\sigma$ . The excess at  $m_{h^0} \approx 115$  GeV/ $c^2$  is discussed in [25]; its significance is also only slightly over  $2\sigma$ .

Due to the large range of models investigated and the fine reconstructed mass resolutions, the probability to have a  $2\sigma$  excess somewhere is much larger than the 5% it would be if only a single counting experiment had been done. Over the range shown in Figure 1, the dilution factor of the significance is estimated to be 30–60. This estimation was performed by scaling the signal and background estimations of DELPHI and OPAL’s test-mass-independent analyses of the 1999 and earlier data<sup>2</sup> by a factor of two, randomly generating candidates according to the background estimations, and for each set of random candidates, performing a confidence level calculation in the  $m_{h^0}$ -max scenario and noting the smallest  $1 - \text{CL}_b$  obtained. The probability of obtaining a particular value of  $1 - \text{CL}_b$  or smaller was estimated and compared against  $1 - \text{CL}_b$ . More than one independent  $2\sigma$  excess is probable.

A more detailed view of the combined  $e^+e^- \rightarrow h^0 A^0$  search results is shown in Figures 2 and 3. In these figures, the values of  $-2 \ln Q$ ,  $1 - \text{CL}_b$  and  $\text{CL}_s$  are shown for  $m_{h^0} \approx m_{A^0}$  and at  $\tan \beta = 20$ , as functions of  $m_{h^0} + m_{A^0}$ . For these models,  $\cos^2(\beta - \alpha) \approx 1$ , and the  $e^+e^- \rightarrow h^0 Z^0$  searches do not contribute. The significance of the excesses with  $m_{h^0} \approx m_{A^0}$  in Figure 1 are seen in the plot of  $1 - \text{CL}_b$ . The quantity  $\text{CL}_s$  is used to exclude the signal hypothesis as a function of the MSSM parameters. The lowest unexcluded values of  $m_{h^0}$  and  $m_{A^0}$  correspond to models with lower values of  $\tan \beta$ , for which  $m_{A^0} \neq m_{h^0}$ , and so these lower bounds cannot be determined from Figure 3.

The 95% CL exclusion contours are shown in Figure 4 for the  $m_{h^0}$ -max scenario, and in Figure 5 for the no-mixing scenario. The results for the large  $\mu$  scenario are discussed separately below. In the no-mixing and  $m_{h^0}$ -max scenarios, limits are shown in four projections: the  $(m_{h^0}, m_{A^0})$  projection, the  $(m_{h^0}, \tan \beta)$  projection, the  $(m_{A^0}, \tan \beta)$  projection, and the  $(m_{H^\pm}, \tan \beta)$  projection.

The observed and expected limits for  $m_{h^0}$  and  $m_{A^0}$  for the  $m_{h^0}$ -max and no-mixing scenarios are given in Table 2. For the no-mixing scenario, the lower bounds on  $m_{h^0}$  and  $m_{A^0}$  are given for  $\tan \beta > 0.7$  to highlight the search sensitivity to heavy Higgs bosons. For  $\tan \beta < 0.7$ , there is an unexcluded region with  $m_{A^0}$  below 40 GeV/ $c^2$  and  $m_{h^0}$  above 65 GeV/ $c^2$ . This region is unexcluded because the  $e^+e^- \rightarrow h^0 Z^0 \rightarrow A^0 A^0 Z^0$  process dominates, and  $\text{Br}(A^0 \rightarrow b\bar{b})$  is suppressed, either kinematically, when  $m_{A^0} < 10$  GeV/ $c^2$ , or because the coupling of the  $A^0$  to  $b\bar{b}$  becomes sufficiently suppressed so that exclusion via b-tagging channels becomes impossible. For unexcluded models in the no-mixing scenario with  $\tan \beta < 0.7$ , the mass of the charged Higgs boson is less than 74 GeV/ $c^2$ . The lower bound obtained by the combination of direct searches at LEP [27] is 78.6 GeV/ $c^2$ . The LEP charged Higgs boson searches assume however that  $\text{Br}(H^+ \rightarrow c\bar{s}) + \text{Br}(H^+ \rightarrow \tau^+ \nu_\tau) = 1$ . This assumption is broken by  $\text{Br}(H^+ \rightarrow W^{*+} A^0)$ , which can be as large as 0.6 for  $\tan \beta = 0.7$  and  $m_{H^\pm} = 74$  GeV/ $c^2$ , at the extremum of the unexcluded area. The decays of both the  $H^+$  and the  $H^-$  have to be considered in signal

<sup>2</sup>Since this estimation was done, OPAL has created new test-mass-dependent analyses for the 1999 data.

events. The LEP-combined limits on the cross-section assuming only fermionic  $H^\pm$  decays are of the order of 20% of the predicted cross-section for  $m_{H^\pm}=74$  GeV/ $c^2$ , and so it is not clear that the entire unexcluded region can be covered by the constraint from charged Higgs boson searches. Additional study is required to quantify the effect of the charged Higgs searches on this scenario.

For models with  $m_{A^0} < 4$  GeV/ $c^2$ , the decay branching fractions of the  $A^0$  are uncertain. In the  $m_{h^0}$ -max scenario for all values of  $m_{h^0}$ , and for the no-mixing scenario for  $m_{h^0} < 65$  GeV/ $c^2$ , however, models with  $m_{A^0} < 4$  GeV/ $c^2$  are excluded regardless of the  $A^0$  decay modes because the production cross-section for  $h^0 Z^0$  multiplied by  $\text{Br}(h^0 \rightarrow b\bar{b})$  provides a sufficient signal to exclude these models. If  $m_{h^0}$  is too low to allow decays to  $b\bar{b}$ , then the additional width to the  $Z^0$  resonance from the  $h^0 Z^0$  process or the  $h^0 A^0$  process would exceed the upper limit on the excess  $Z^0$  width [36].

Scenario	$m_{h^0}$ limit (GeV/ $c^2$ )	$m_{A^0}$ limit (GeV/ $c^2$ )	Excluded $\tan \beta$ observed limit (expected limit)
$m_{h^0}$ -max	91.0 (94.6)	91.9 (95.0)	$0.5 < \tan \beta < 2.4$ ( $0.5 < \tan \beta < 2.6$ )
No Mixing	91.5 (95.0)	92.2 (95.3)	$0.7 < \tan \beta < 10.5$ ( $0.8 < \tan \beta < 16.0$ )

Table 2: Limits on  $m_{h^0}$  and  $m_{A^0}$  in the  $m_{h^0}$ -max and no-mixing benchmark scenarios explained in the text. The median expected limits in an ensemble of SM background-only experiments are listed in parentheses. To highlight the sensitivity of the searches for massive Higgs bosons, the limits on  $m_{h^0}$  and  $m_{A^0}$  are given with the additional constraint of  $\tan \beta > 0.7$  for the no-mixing scenario. If  $\tan \beta$  is explored in the full region to 0.4, then values of  $m_{A^0}$  below 40 GeV/ $c^2$  are not excluded for values of  $m_{h^0}$  above 65 GeV/ $c^2$  in the no-mixing scenario. The excluded regions for the  $m_{h^0}$ -max and no-mixing scenarios are shown in Figures 4 and 5.

The searches presented here allow regions of  $\tan \beta$  to be excluded within the contexts of the  $m_{h^0}$ -max and no-mixing scenarios. For the  $m_{h^0}$ -max scenario, values of  $\tan \beta$  between 0.5 and 2.4 are excluded, while for the no mixing scenario, values of  $\tan \beta$  between 0.7 and 10.5 are excluded. The  $\tan \beta$  limits in the  $m_{h^0}$ -max scenario are determined by the exclusion limit for the  $h^0 Z^0$  process, which depends strongly on the centre-of-mass energies LEP achieved. For the no-mixing scenario, the  $\tan \beta$  limits are more complex. The lower limit is determined by the lack of sensitivity to the processes  $e^+e^- \rightarrow h^0 Z^0 \rightarrow A^0 A^0 Z^0$ , where the  $A^0$  does not decay to  $b\bar{b}$  either because  $\tan \beta$  is too small or because the  $A^0$  is too light. The upper limit is determined by the kinematic sensitivity of the  $e^+e^- \rightarrow h^0 A^0$  searches which leave an unexcluded region for  $90 < m_{A^0} < 120$  GeV. In this region, where Higgsstrahlung is suppressed by the small value of  $\sin^2(\beta - \alpha)$  and  $e^+e^- \rightarrow h^0 A^0$  is kinematically out of reach, the maximum value of  $m_{H^0}$  is 114.6 GeV. However, including the sensitivity to  $e^+e^- \rightarrow H^0 Z^0$  production does not improve the limits because models with  $m_{H^0}$  between 114.1 GeV and 114.6 GeV exist near the limits that are set. The uncertainty on the model also does not encourage the use of the Heavy Higgs signal to place limits on  $\tan \beta$ .

The region with  $m_{A^0} > 300$  GeV in the no-mixing scenario also has an unexcluded portion at high  $\tan \beta$  due to the fact that the limit in the Standard Model ( $h^0 Z^0$ ) searches is 114.1 GeV [25], while the maximum possible value of  $m_{h^0}$  in this scenario is 114.3 GeV. This region at high  $m_{A^0}$  does not contribute to the  $\tan \beta$  limit because it is at higher  $\tan \beta$  than the region at lower  $m_{A^0}$ . If the model were to allow even slightly higher maximal



values of  $m_{h^0}$  in the no-mixing scenario, then the upper value of the  $\tan\beta$  limit could be reduced because unexcluded regions will appear at high  $m_{A^0}$ ; it is for this reason that the upper limit on  $\tan\beta$  in this scenario is rather uncertain.

In a more general scan, where the MSSM parameters are varied independently and the top quark mass is allowed to be larger, the limits on  $m_{h^0}$ ,  $m_{A^0}$  and  $\tan\beta$  are weaker (see the discussions, for example, of Ref. [34]). In particular, if the mass of the top quark is  $179 \text{ GeV}/c^2$  (roughly  $1\sigma$  higher than measured central value), then  $\tan\beta$  can no longer be excluded above 1.9 or below 0.6 in the  $m_{h^0}$ -max scenario.

### 3.2.2 The Large $\mu$ Scenario

The combination of the four experiments' results in the large  $\mu$  scenario now includes the flavour-independent  $e^+e^- \rightarrow h^0 Z^0$  searches with  $h^0 \rightarrow \text{hadrons}$  [16–21]. In all cases, the cross-sections and decay branching ratios are computed with SUBHPOLE2 [5]. Because of the large overlaps of the accepted signals, backgrounds, and the observed candidates between the flavour-independent searches with the corresponding b-tagged searches, only one set of searches is considered for each set of parameters in the scenario, choosing between the flavour-independent set and the b-tagged set the channels which yield the best expected sensitivity, given by the smallest median  $\text{CL}_s$  in the background-only hypothesis. The previous combination [37] of the LEP search results, which only included channels relying<sup>3</sup> on  $h^0$  decays to  $b\bar{b}$  and to  $\tau^+\tau^-$ , did not exclude some choices of  $m_{A^0}$  and  $\tan\beta$ . For the unexcluded models, the signal events, while plentiful, were not selected because the leading decay branching ratios of the  $h^0$  are to  $c\bar{c}$ , gluons and  $W^+W^-$ ; the  $b\bar{b}$  decays are suppressed by the choice of model parameters and there is an insufficient branching ratio of the  $h^0$  to  $\tau^+\tau^-$ .

Because the light Higgs boson  $h^0$  has a mass less than  $108 \text{ GeV}/c^2$  for all choices of  $(m_{A^0}, \tan\beta)$  in this model, and because  $e^+e^- \rightarrow H^0 Z^0$  is within kinematic reach whenever  $e^+e^- \rightarrow h^0 Z^0$  is suppressed by a small  $\sin^2(\beta - \alpha)$  and  $m_{h^0} + m_{A^0} > \sqrt{s}$ , there is always a Higgs signal with sizeable strength for all considered models within the large  $\mu$  scenario. The challenge of this scenario is to test models with non- $b\bar{b}$  and non- $\tau^+\tau^-$  decay modes.

A careful scan over the model space indicates that the addition of the flavour-independent  $e^+e^- \rightarrow h^0 Z^0$  searches adds enough sensitivity to exclude the models which were previously unexcluded, although for some model points they are interpreted as flavour-independent  $e^+e^- \rightarrow H^0 Z^0$  searches. This scenario is therefore entirely excluded at the 95% confidence level.

## 3.3 Coupling Strength Limits

Searches for  $h^0 A^0$  production with reduced cross-sections or branching ratios compared to those predicted in the MSSM scenarios investigated here are of great interest. More stringent limits on the  $h^0 A^0$  production cross-section allow tests of models which either predict lower cross-sections or reduced branching ratios of the Higgs bosons to the final states which are sought at LEP. Examples of such models are those involving substantial CP-violation in the MSSM Higgs sector [39] and general two-Higgs-doublet models (2HDMs) without SUSY constraints [40].

---

<sup>3</sup>The ALEPH leptonic and missing-energy Standard Model Higgs channels have some sensitivity to non- $b\bar{b}$  Higgs boson decays, but they are not optimised for the flavour-blind interpretations, and more sensitivity is needed to exclude some models in the large  $\mu$  scenario.

The  $e^+e^- \rightarrow h^0 A^0$  search results from the four experiments are combined using the MSSM model considered in the  $m_{h^0}$ -max scenario above to compute the dependence of the  $e^+e^- \rightarrow h^0 A^0$  cross-section on the centre-of-mass energy. The coupling limits are produced separately for the set of  $h^0 A^0 \rightarrow b\bar{b}b\bar{b}$  search channels, for the set of  $h^0 A^0 \rightarrow b\bar{b}\tau^+\tau^-$  search channels, and also for a combination of all  $h^0 A^0$  search channels assuming fixed branching ratios. The branching ratios chosen for the third set of coupling limits is  $\text{Br}(h^0 \rightarrow b\bar{b})=0.94$ ,  $\text{Br}(A^0 \rightarrow b\bar{b})=0.92$ ,  $\text{Br}(h^0 \rightarrow \tau^+\tau^-)=0.06$  and  $\text{Br}(A^0 \rightarrow \tau^+\tau^-)=0.08$ , which are typical in the  $m_{h^0}$ -max scenario for values of  $\tan\beta$  greater than 10. In all cases,  $\cos^2(\beta - \alpha) = 1$ , and the signal is multiplied by a scale factor such that the scaled signal is excluded at exactly the 95% confidence level ( $\text{CL}_s = 0.05$ ). Presently, no  $h^0 A^0 \rightarrow \tau^+\tau^-\tau^+\tau^-$  searches are combined. The coupling strength limits for the three combinations of channels are shown in Figures 6 through 8. These limits can be interpreted as upper bounds on  $\cos^2(\beta - \alpha)\text{Br}(h^0 \rightarrow b\bar{b})\text{Br}(A^0 \rightarrow b\bar{b})$ ,  $\cos^2(\beta - \alpha)\text{Br}(h^0 \rightarrow b\bar{b})\text{Br}(A^0 \rightarrow \tau^+\tau^-)$ , and  $\cos^2(\beta - \alpha)$  assuming the fixed branching ratios mentioned above. The limits for the  $b\bar{b}\tau^+\tau^-$  channels can be interpreted for either the  $h^0$  or the  $A^0$  decaying into  $\tau^+\tau^-$ , while the other decays to  $b\bar{b}$ . The experimental limits are shown in the figures along with the limits that are expected in an ensemble of hypothetical experiments in which there is no signal.

## Acknowledgements

We congratulate our colleagues for the LEP Accelerator Division for the successful running in the year 2000 at the highest energies, and would like to express our thanks to the engineers and technicians in all our institutions for their contributions to the excellent performance of the four LEP experiments. The LEP Higgs working group acknowledges the fruitful cooperation between the experiments in exchanging the experimental results and developing and applying procedures for combining them.

## References

- [1] Y. Okada, M. Yamaguchi and T. Yanagida, *Prog. Theor. Phys.* **85** (1991) 1.
- [2] J. Ellis, G. Ridolfi and F. Zwirner, *Phys. Lett.* **B257** (1991) 83.
- [3] H.E. Haber and R. Hempfling, *Phys. Rev. Lett.* **66** (1991) 1815.
- [4] M. Carena, J. R. Espinosa, M. Quirós and C.E.M. Wagner, *Phys. Lett.* **B355** (1995) 209.
- [5] M. Carena, M. Quirós and C.E.M. Wagner, *Nucl. Phys.* **B461** (1996) 407.
- [6] H.E. Haber, R. Hempfling and A.H. Hoang, *Zeit für Phys.* **C75** (1997) 539.
- [7] S. Heinemeyer, W. Hollik and G. Weiglein, *Eur. Phys. Jour.* **C9** (1999) 343.
- [8] J. R. Espinosa and R. Zhang, *Nucl. Phys.* **B586** (2000) 3.
- [9] ALEPH Collab., R. Barate *et al.*, *Phys. Lett.* **B495** (2000) 1.
- [10] DELPHI Collab., P. Abreu *et al.*, *Phys. Lett.* **B499** (2001) 23.

- [11] L3. Collab., “Search for the Standard Model Higgs Boson with the L3 Experiment at LEP”, L3 Note 2688, June 2001. Submitted to Phys. Lett. B.
- [12] OPAL Collab., published in Phys. Lett. **B499** (2001) 38.
- [13] ALEPH Collab., “Searches for neutral Higgs bosons of the MSSM at centre-of-mass energies up to 209 GeV with the ALEPH detector at LEP”, ALEPH 2001-022 CONF 2001-019, 6 March, 2001.
- [14] DELPHI Collab., “Searches for neutral supersymmetric Higgs bosons in  $e^+e^-$  collisions up to  $\sqrt{s} = 209$  GeV”, DELPHI 2001-070 CONF 498, 4 July, 2001.
- [15] L3 Collab., “Search for Neutral Higgs Bosons of the Minimal Supersymmetric Standard Model in  $e^+e^-$  Interactions at  $\sqrt{s}$  up to 209 GeV”, L3 Note 2692, July 2001.
- [16] OPAL Collab., “Searches for Higgs Bosons in Extensions to the Standard Model in  $e^+e^-$  Collisions at the Highest LEP Energies” OPAL Physics Note PN472, 27 February, 2001.
- [17] ALEPH Collab., “A flavour-independent search for the Higgsstrahlung process in  $e^+e^-$  collisions at centre-of-mass energies from 189 to 209 GeV”, ALEPH 2001-021 CONF 2001-018.
- [18] DELPHI Collab., “Generalised Search for Hadronic Decays of Higgs Bosons with the DELPHI Detector at LEP-2”, DELPHI 2001-070 CONF 498, July 2001.
- [19] L3 Collab., “Flavour Independent Search for Hadronically Decaying Higgs Boson in Higgs-strahlung Process at  $\sqrt{s}$  up to 209 GeV”, L3 Note 2693, July 2001.
- [20] OPAL Collab., Eur. Phys. J. **C18** (2001) 425;  
OPAL Collab., “Model Independent Searches for Scalar Bosons with the OPAL Detector at LEP”, Physics Note PN449, available at <http://opal.web.cern.ch/Opal/pubs/physnote/info/pn449.html>.
- [21] The ALEPH, DELPHI, L3 and OPAL Collaborations, and the LEP Higgs Working Group, “Generalised Search for Hadronic Decays of Higgs Bosons at LEP-2”, LEP Higgs WG Note 2001-07, July, 2001.
- [22] HZHA generator: P. Janot, in “Physics at LEP2”, edited by G. Altarelli, T. Sjöstrand and F. Zwirner, CERN 96-01 Vol. 2 p.309.  
For HZHA3 and HZHA2, see <http://alephwww.cern.ch/~janot/Generators.html>.
- [23] S. Heinemeyer, W. Hollik and G. Weiglein, Phys. Rev. **D58** (1998) 091701, Phys. Lett. **B440** (1998) 296, hep-ph/9807423 and JHEP 0006 (2000) 009.
- [24] S. Heinemeyer, W. Hollik and G. Weiglein, Comp. Phys. Comm. **124** (2000) 76; Also see <http://www.feynhiggs.de>.
- [25] The ALEPH, DELPHI, L3 and OPAL Collaborations, and the LEP Higgs Working Group, “Search for the Standard Model Higgs Boson at LEP”, LEP Higgs WG Note 2001-03, July 2001.
- [26] R. D. Cousins and V. L. Highland, Nucl. Instr. Meth **A320** (1992) 331.

- [27] ALEPH, DELPHI, L3 and OPAL Collaborations, and the LEP Higgs Working Group, “Search for Charged Higgs boson: Preliminary combined results using LEP data collected at energies up to 209 GeV” LEP Higgs WG Note 2001-05.
- [28] ALEPH, DELPHI, L3, OPAL Collab., and the LEP working group for the Higgs boson searches, “Search for Higgs bosons: Preliminary combined results using LEP data collected at energies up to 202 GeV,” CERN-EP/2000-055, 25 Apr 2000.
- [29] D.E. Groom *et al*, Eur. Phys. Jour. **C15** (2000) 1, available on the PDG WWW pages (URL: <http://pdg.lbl.gov/>).
- [30] M. Carena, S. Heinemeyer, C. E. M. Wagner and G. Weiglein, hep-ph/9912223.
- [31] M. Carena, S. Mrenna and C. Wagner, Phys. Rev. D60 (1999) 075010.
- [32] M. Carena, H. E. Haber, S. Heinemeyer, W. Hollik, C. E. M. Wagner and G. Weiglein, Nucl. Phys. **B580** (2000) 29.
- [33] J. R. Espinosa and R.-J. Zhang, JHEP 0003:026 (2000).
- [34] OPAL Collab., G. Abbiendi *et al.*, Eur. Phys. J. **C12** (2000) 567-586.
- [35] The ALEPH, DELPHI, L3 and OPAL Collaborations, and the LEP Higgs Working Group, “Searches for Higgs Bosons: Preliminary Combined Results from the Four LEP Experiments at  $\sqrt{s} \approx 189$  GeV, ALEPH 99-081 CONF 99-052, DELPHI 99-142 CONF 327, L3 Note 2442, OPAL Technical Note TN614, July 1999.
- [36] The ALEPH, DELPHI, L3 and OPAL Collaborations, the LEP Electroweak Working Group, and the SLD Heavy Flavour and Electroweak Groups, “A Combination of Preliminary Electroweak Measurements and Constraints on the Standard Model”, LEPEWWG/2001-01, May 2001.
- [37] ALEPH, DELPHI, L3 and OPAL Collaborations, and the LEP Higgs Working Group, “Searches for the Neutral Higgs Bosons of the MSSM: Preliminary Combined Results using LEP Data Collected at Energies up to 209 GeV”, LHWG note 2001-02.
- [38] A. G. Akeroyd and W. J. Stirling, Nucl. Phys. **B447** (1995), 3.
- [39] M. Carena, J. Ellis, A. Pilaftsis and C. Wagner, Nucl. Phys. **B586** (2000) 92.
- [40] J. Gunion, H. Haber, G. Kane and S. Dawson, *The Higgs Hunter’s Guide*, Addison-Wesley Publishing Company (1990).

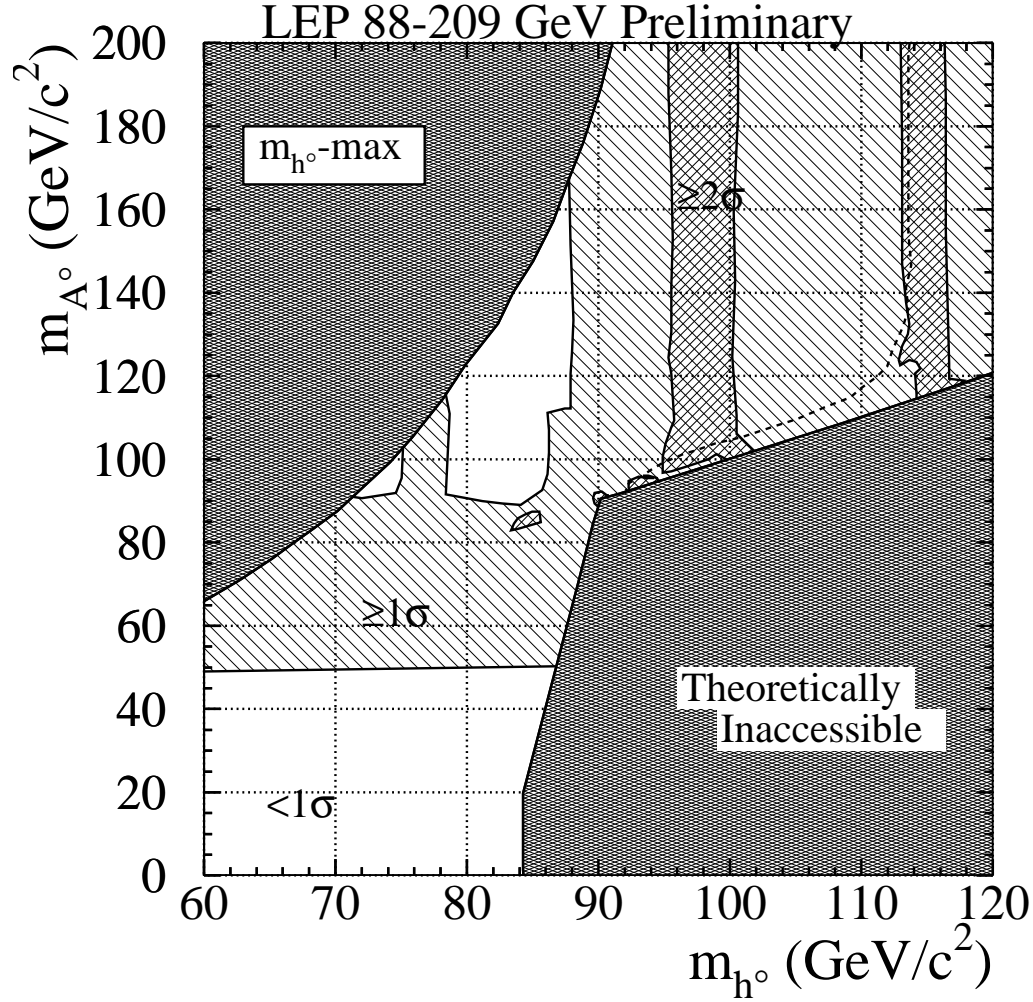


Figure 1: The distribution of the confidence level  $CL_b$  in the  $(m_{h^0}, m_{A^0})$  plane for the  $m_{h^0}$ -max scenario. In the white domain, the observation either shows a deficit or is less than  $1\sigma$  above the background prediction, while in the domains labelled  $\geq 1\sigma$  and  $\geq 2\sigma$ , the observation shows an excess above the SM background prediction ( $1 - CL_b < 0.32$ ,  $1 - CL_b < 0.05$ , respectively). If at a point  $(m_{h^0}, m_{A^0})$  in the plane, two values of  $\tan\beta$  are allowed by the benchmark model, the choice of  $\tan\beta$  with the smaller  $1 - CL_b$  is shown. Results from the  $h^0Z^0$  searches are combined with the results of the  $h^0A^0$  searches. Vertical structures are due to features in the  $h^0Z^0$  search results, while structure on the  $m_{h^0}=m_{A^0}$  line arises from the  $h^0A^0$  searches. The 95% CL exclusion contour is shown with the dashed line; points to the right and below the dashed line are unexcluded. These regions can also be seen in Figure 4.

## LEP 88-209 GeV Preliminary

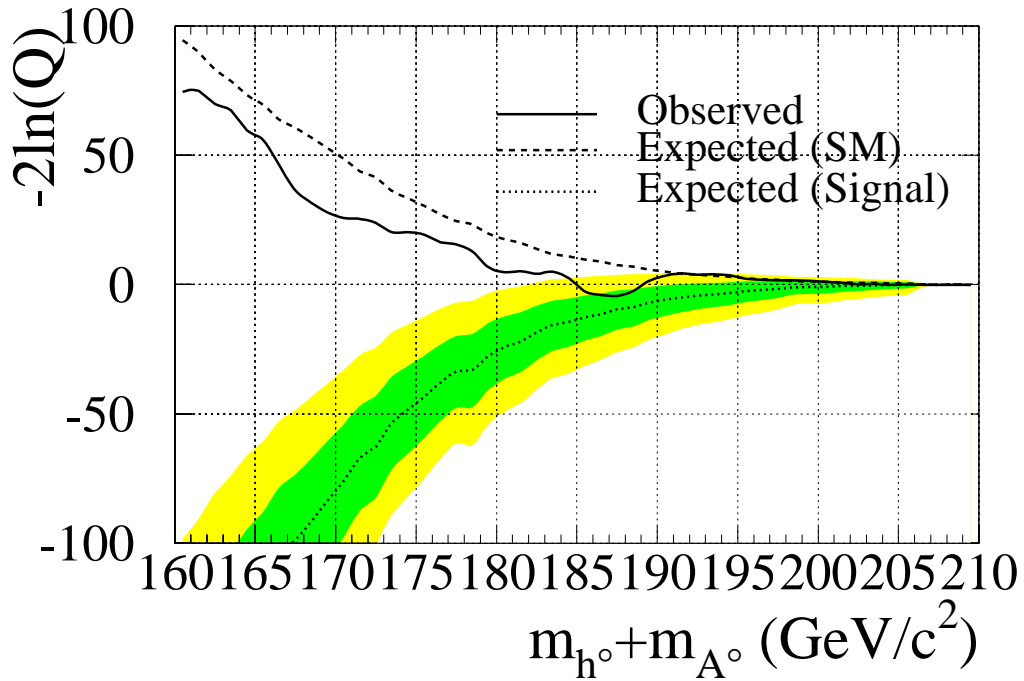


Figure 2: The value of the likelihood ratio  $-2\ln Q$  as a function of the sum of the test masses  $m_{h^0} + m_{A^0}$ , for  $m_{h^0} \approx m_{A^0}$  ( $\tan\beta > 20$ ,  $\cos^2(\beta - \alpha) \approx 1$ ) in the  $m_{h^0}$ -max scenario. The solid curve shows the observed values of  $-2\ln Q$  in the combination of the four experiments' results; the upper dashed curve shows the median expectations in an ensemble of hypothetical experiments in which only Standard Model background processes contribute, and the lower dotted curve shows the median expectations in an ensemble of hypothetical experiments in which a signal is also present. The dark-shaded band indicates the 68% probability region centred on the median signal+background expectation, while the light-shaded band indicates the 95% probability region.

### LEP 88-209 GeV Preliminary

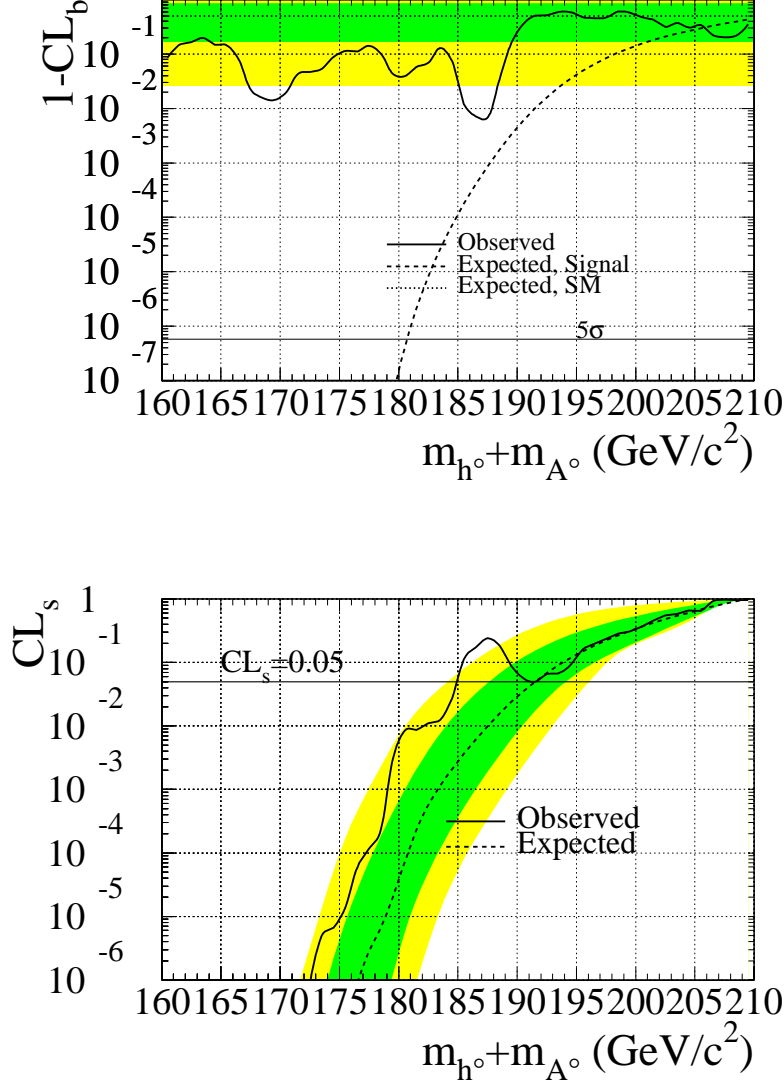


Figure 3: The values of  $1 - \text{CL}_b$  and  $\text{CL}_s$  for the  $m_{h^0} \approx m_{A^0}$  diagonal ( $\tan \beta > 20$ ,  $\cos^2(\beta - \alpha) \approx 1$ ) in the  $m_{h^0}$ -max scenario. The top plot shows the observed value of  $1 - \text{CL}_b$  as a function of  $m_{h^0} + m_{A^0}$  in this scenario, as well as its median expected value (dashed line) in the presence of a signal at the test mass. The value of  $1 - \text{CL}_b$  is expected to be uniformly distributed between zero and one if there is no signal present. The dark shaded band is the 68% probability region centred on  $1 - \text{CL}_b = 0.5$ , and the light-shaded band is the 95% probability region centred also on  $1 - \text{CL}_b = 0.5$ . The solid line labelled “5σ” is drawn at  $1 - \text{CL}_b = 5.7 \times 10^{-7}$ . In the lower plot, the observed value of  $\text{CL}_s$  is shown in the same scenario for the same high- $\tan \beta$  models. The median expected  $\text{CL}_s$  in an ensemble of background-only experiments is shown with a dashed line, and 68% and 95% probability contours are shown with dark and light shading, respectively. Models with  $\text{CL}_s < 0.05$  are excluded at the 95% confidence level. The lowest unexcluded values of  $m_{h^0}$  and  $m_{A^0}$  correspond to models with lower values of  $\tan \beta$ , for which  $m_{A^0} \neq m_{h^0}$ .

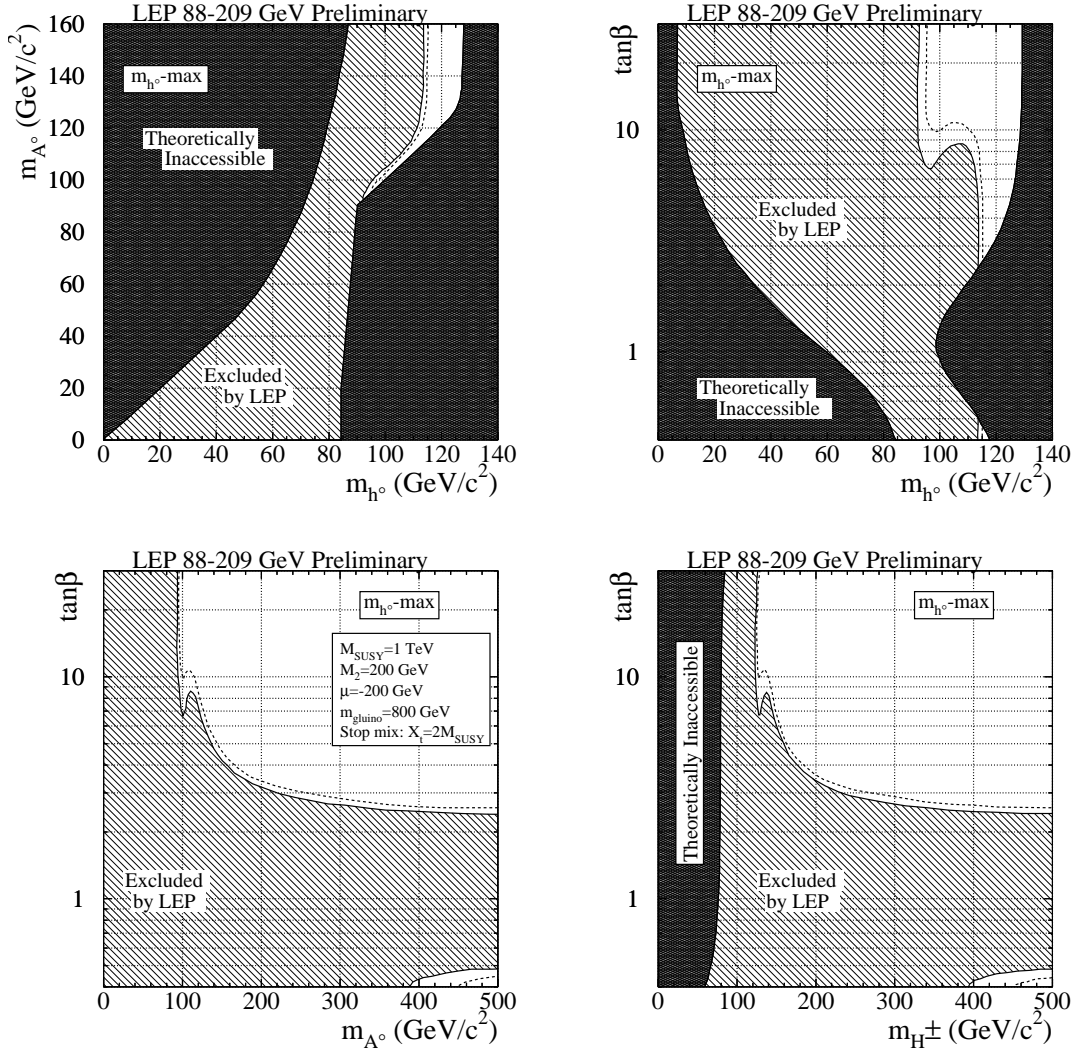


Figure 4: The MSSM exclusion for the  $m_{h^0}$ -max benchmark scenario described in the text of Section 3. This figure shows the excluded (diagonally hatched) and theoretically disallowed (cross-hatched) regions as functions of the MSSM parameters in four projections: (upper left) the  $(m_{h^0}, m_{A^0})$  plane, (upper right) the  $(m_{h^0}, \tan\beta)$  plane, (lower left) the  $(m_{A^0}, \tan\beta)$  plane and (lower right) the  $(m_{H^\pm}, \tan\beta)$  plane. The dashed lines indicate the boundaries of the regions expected to be excluded at the 95% CL if only SM background processes are present.



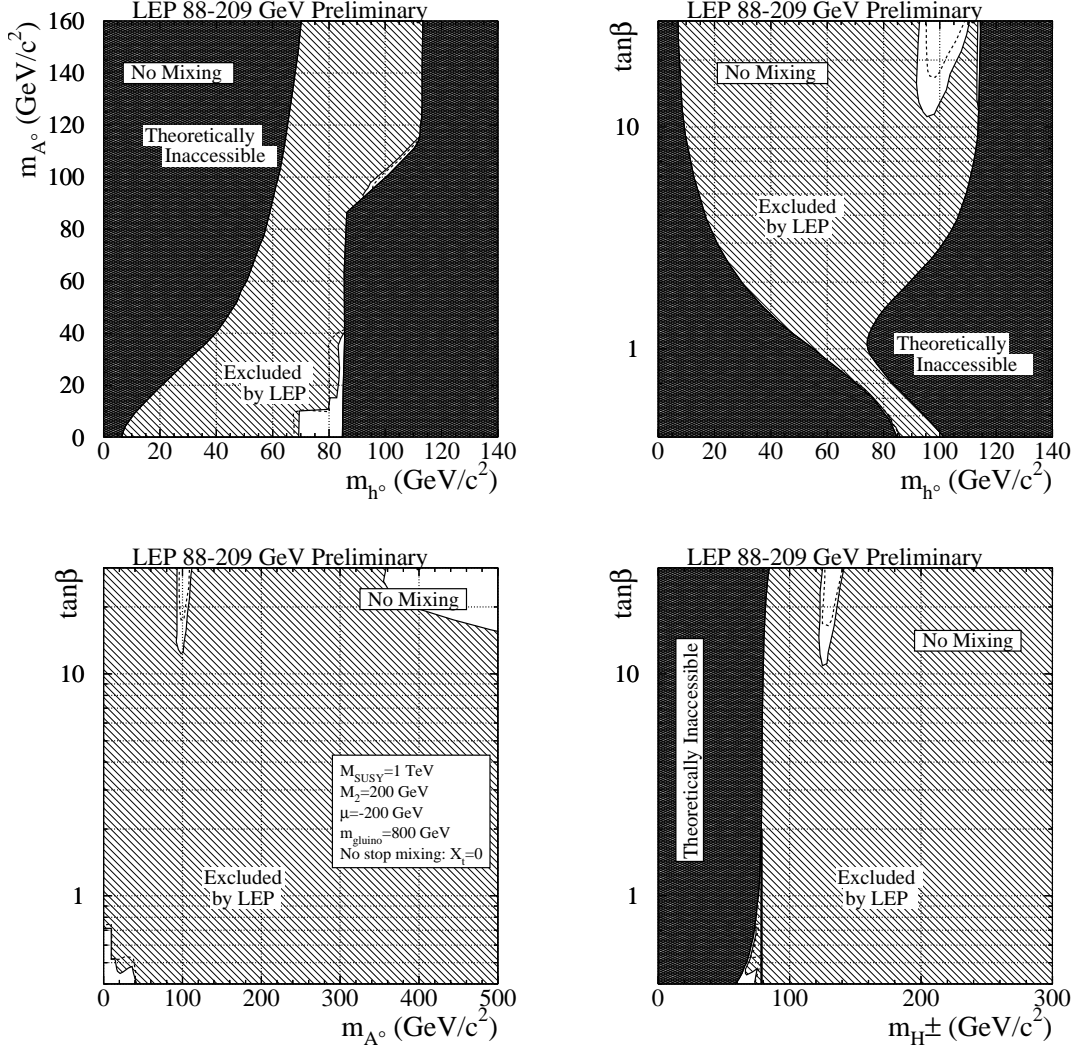


Figure 5: The MSSM exclusion for the “no mixing” benchmark scenario described in the text of Section 3. This figure shows the excluded (diagonally hatched) and theoretically inaccessible (cross-hatched) regions as functions of the MSSM parameters in four projections: (upper left) the  $(m_{h^0}, m_{A^0})$  plane, (upper right) the  $(m_{h^0}, \tan\beta)$  plane, (lower left) the  $(m_{A^0}, \tan\beta)$  plane and (lower right) the  $(m_{H^\pm}, \tan\beta)$  plane. The dashed lines indicate the boundaries of the regions expected to be excluded at the 95% CL if only SM background processes are present. In the  $(m_{H^\pm}, \tan\beta)$  projection, a dark vertical line is drawn at  $m_{H^\pm}=78.6$   $\text{GeV}/c^2$ , the lower bound obtained from direct searches at LEP. Due to the decays  $H^\pm \rightarrow W^{*\pm} A^0$ , however, models with  $m_{H^\pm} < 74$  may not be excluded by the direct searches. More study is needed to make a quantitative estimation of the impact of the  $H^\pm$  searches on this scenario.

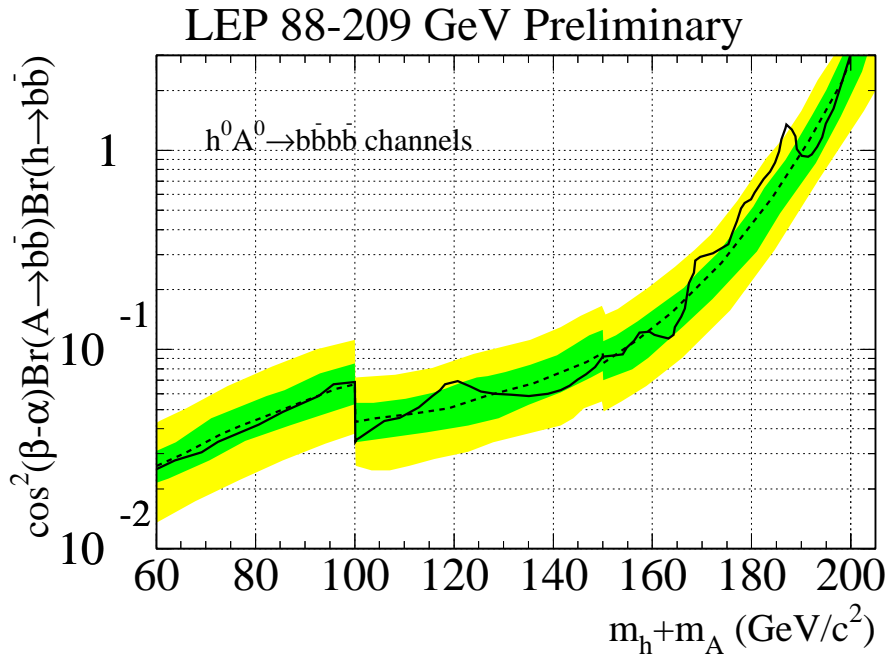


Figure 6: Limit on  $\cos^2(\beta - \alpha) \text{Br}(h^0 \rightarrow b\bar{b}) \text{Br}(A^0 \rightarrow b\bar{b})$ , assuming  $m_{h^0} \approx m_{A^0}$ , and the energy-dependence of the  $e^+e^- \rightarrow h^0 A^0$  cross-section from the  $m_{h^0}$ -max scenario. The solid line is the observed limit, and the dashed line is the median expected limit in an ensemble of hypothetical experiments in the absence of a signal. Contours indicating the 68% and 95% probability bands centred on the median expectation show the expected variation of the limit in an ensemble of background-only experiments.

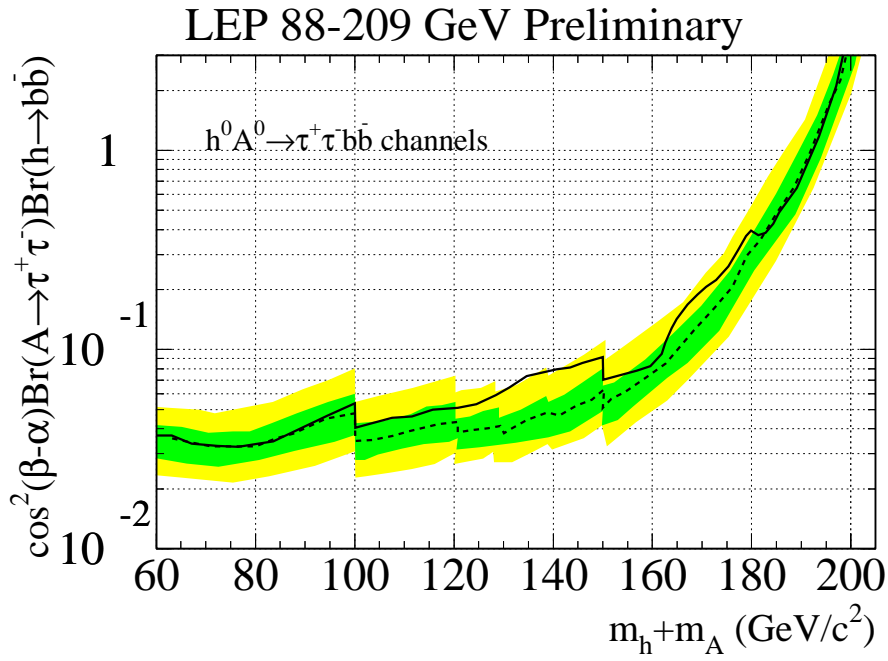


Figure 7: Limit on  $\cos^2(\beta - \alpha) \text{Br}(h^0 \rightarrow b\bar{b}) \text{Br}(A^0 \rightarrow \tau^+ \tau^-)$ , assuming  $m_{h^0} \approx m_{A^0}$  and the energy-dependence of the  $e^+e^- \rightarrow h^0 A^0$  cross-section from the  $m_{h^0}$ -max scenario. The solid line is the observed limit, and the dashed line is the median expected limit in an ensemble of hypothetical experiments in the absence of a signal. Contours indicating the 68% and 95% probability bands centred on the median expectation show the expected variation of the limit in an ensemble of background-only experiments.

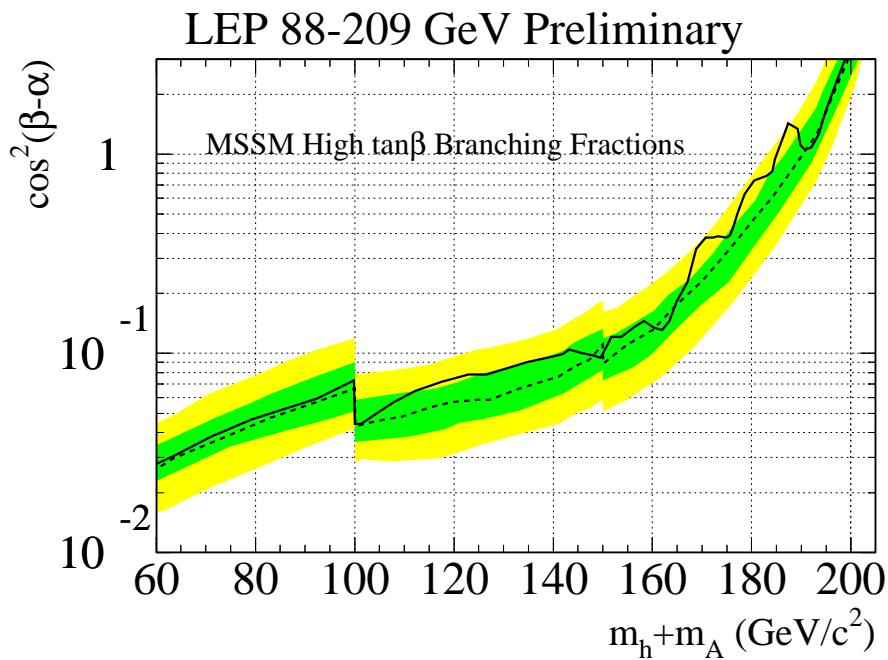
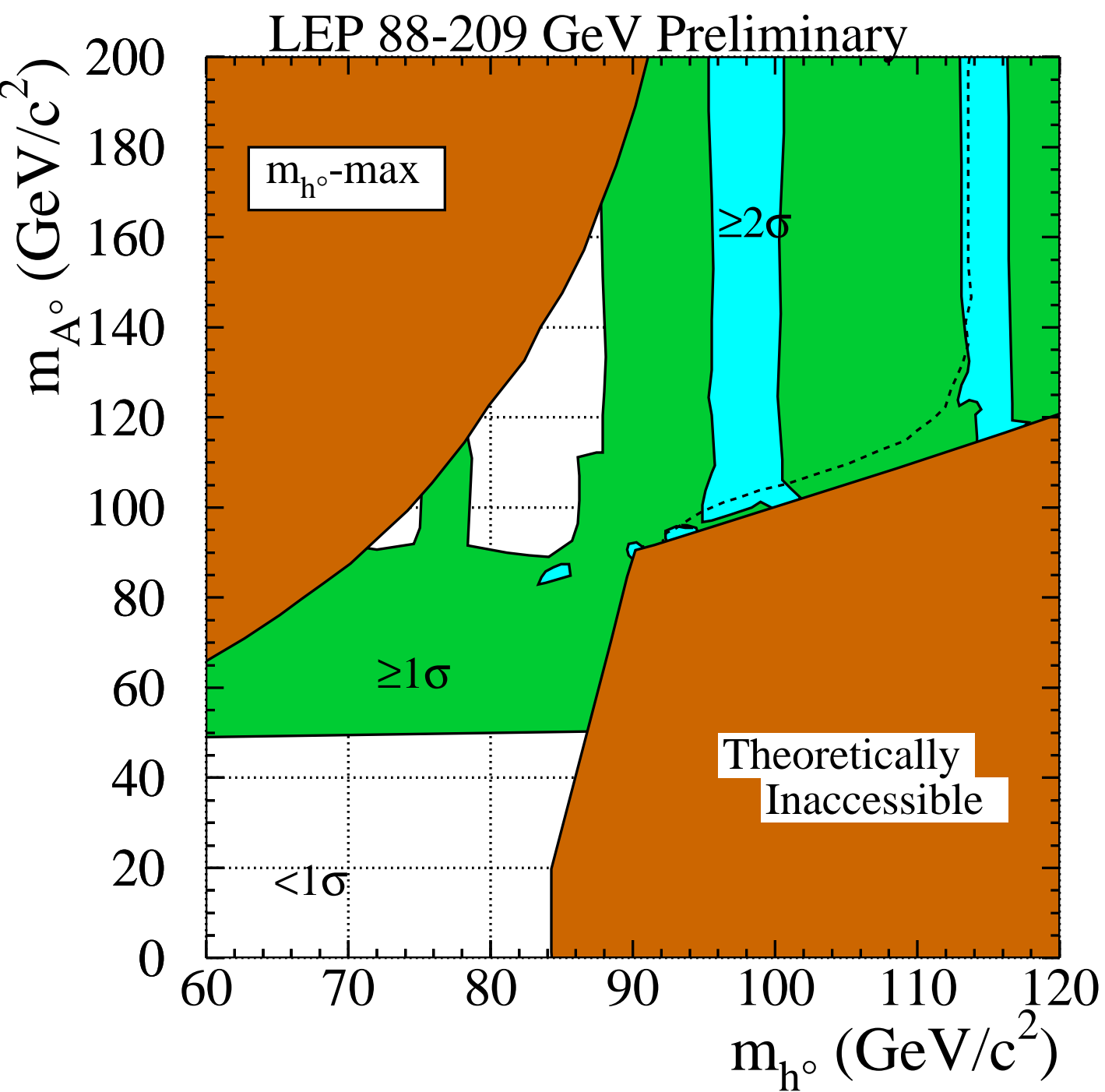
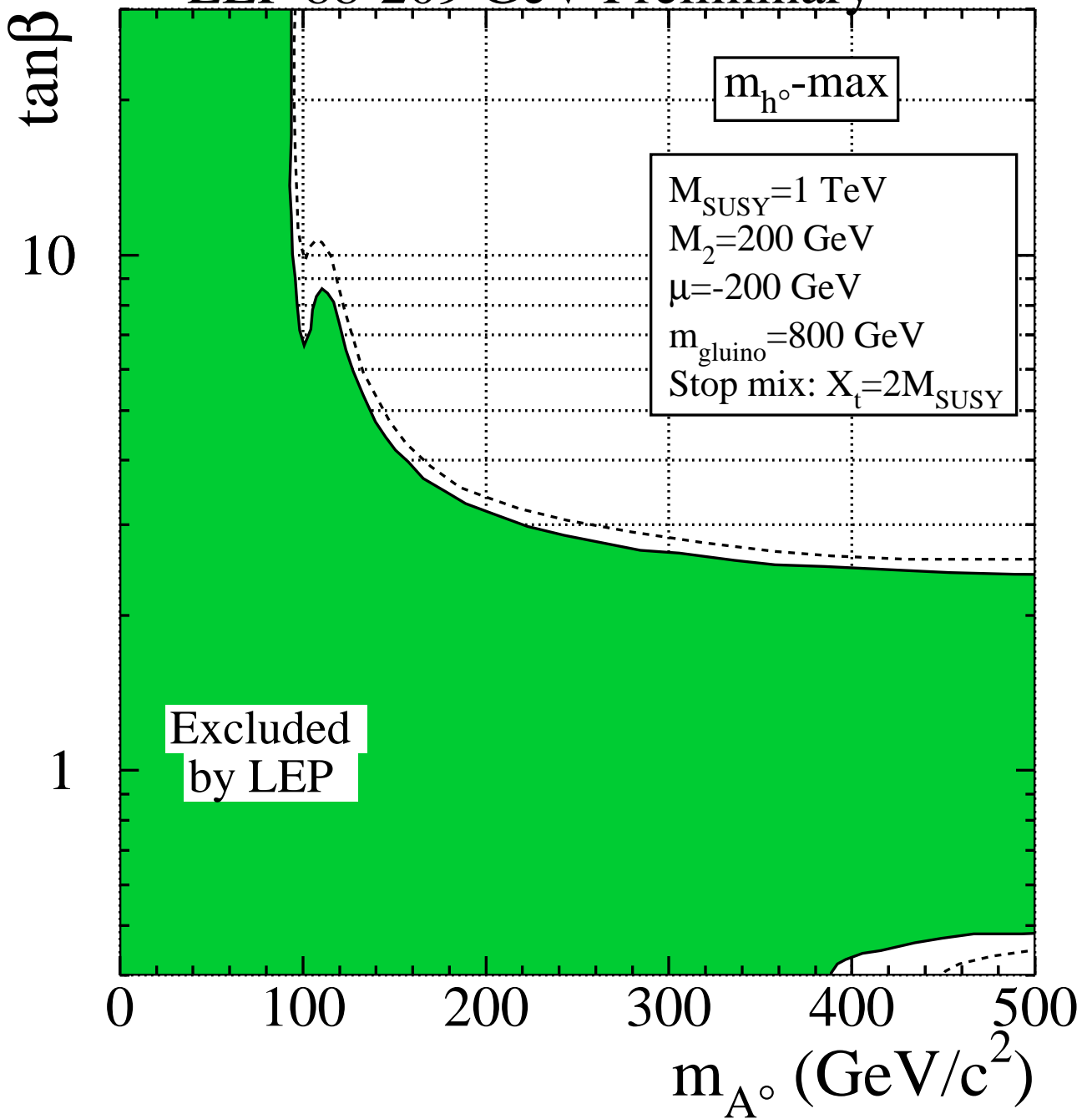


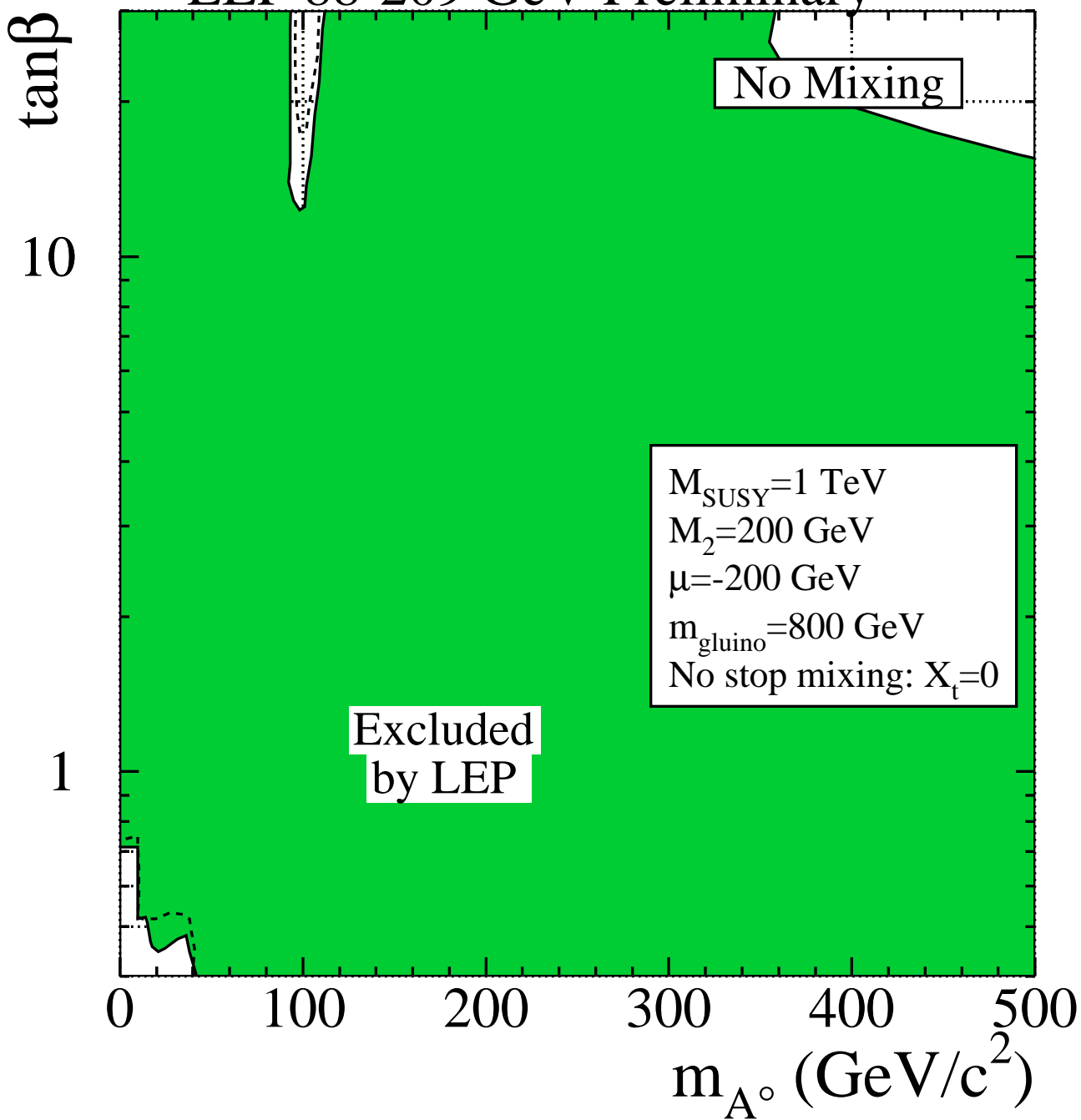
Figure 8: Limit on  $\cos^2\beta - \alpha$ , assuming  $m_{h^0} \approx m_{A^0}$ , and the fixed branching fractions  $\text{Br}(h^0 \rightarrow b\bar{b})=0.94$ ,  $\text{Br}(A^0 \rightarrow b\bar{b})=0.92$ ,  $\text{Br}(h^0 \rightarrow \tau^+\tau^-)=0.06$  and  $\text{Br}(A^0 \rightarrow \tau^+\tau^-)=0.08$ , typical of the  $m_{h^0}$ -max scenario for values of  $\tan\beta$  greater than 10. The solid line is the observed limit, and the dashed line is the median expected limit in an ensemble of hypothetical experiments in the absence of a signal. Contours indicating the 68% and 95% probability bands centred on the median expectation show the expected variation of the limit in an ensemble of background-only experiments.



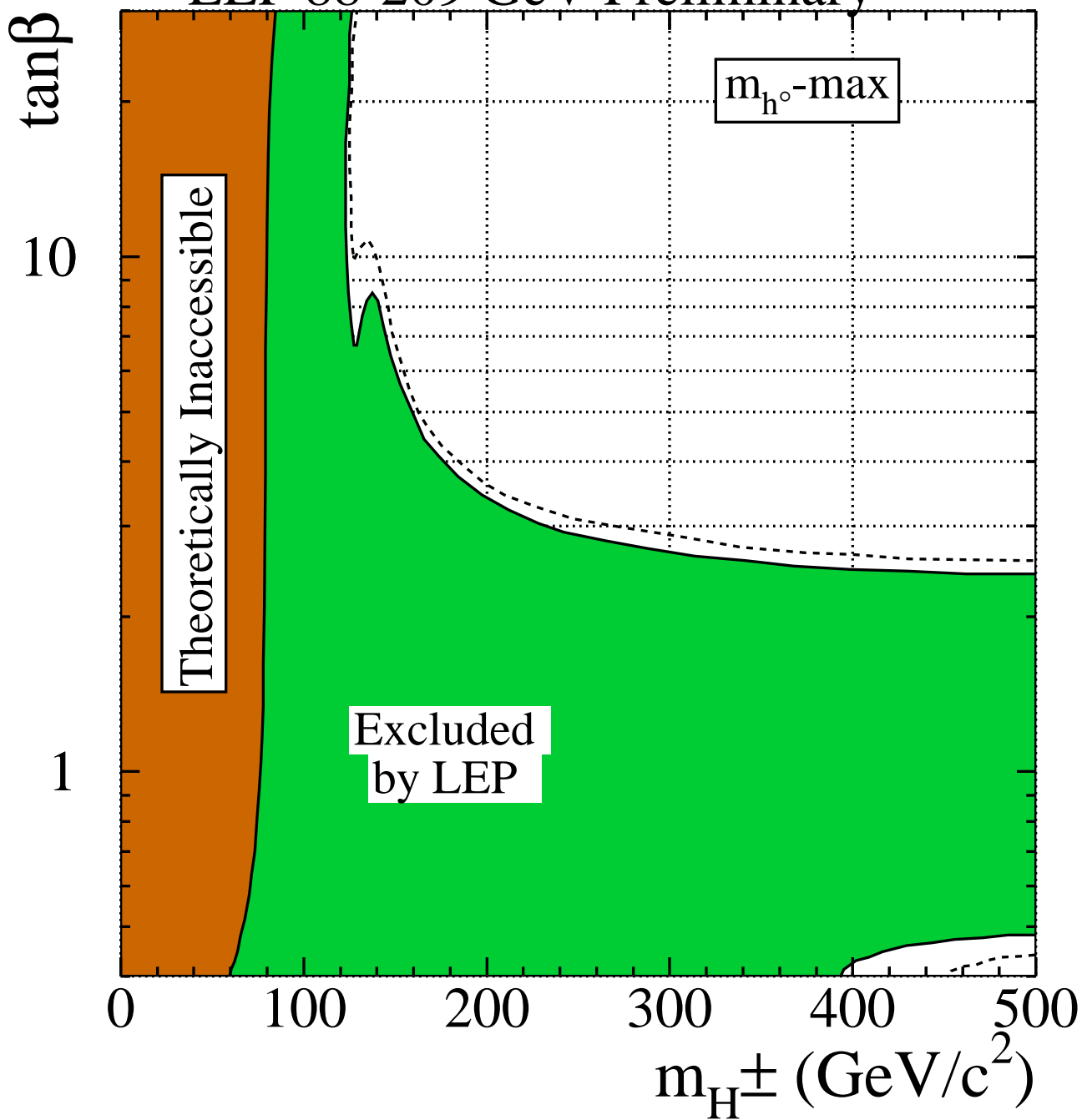
LEP 88-209 GeV Preliminary



LEP 88-209 GeV Preliminary

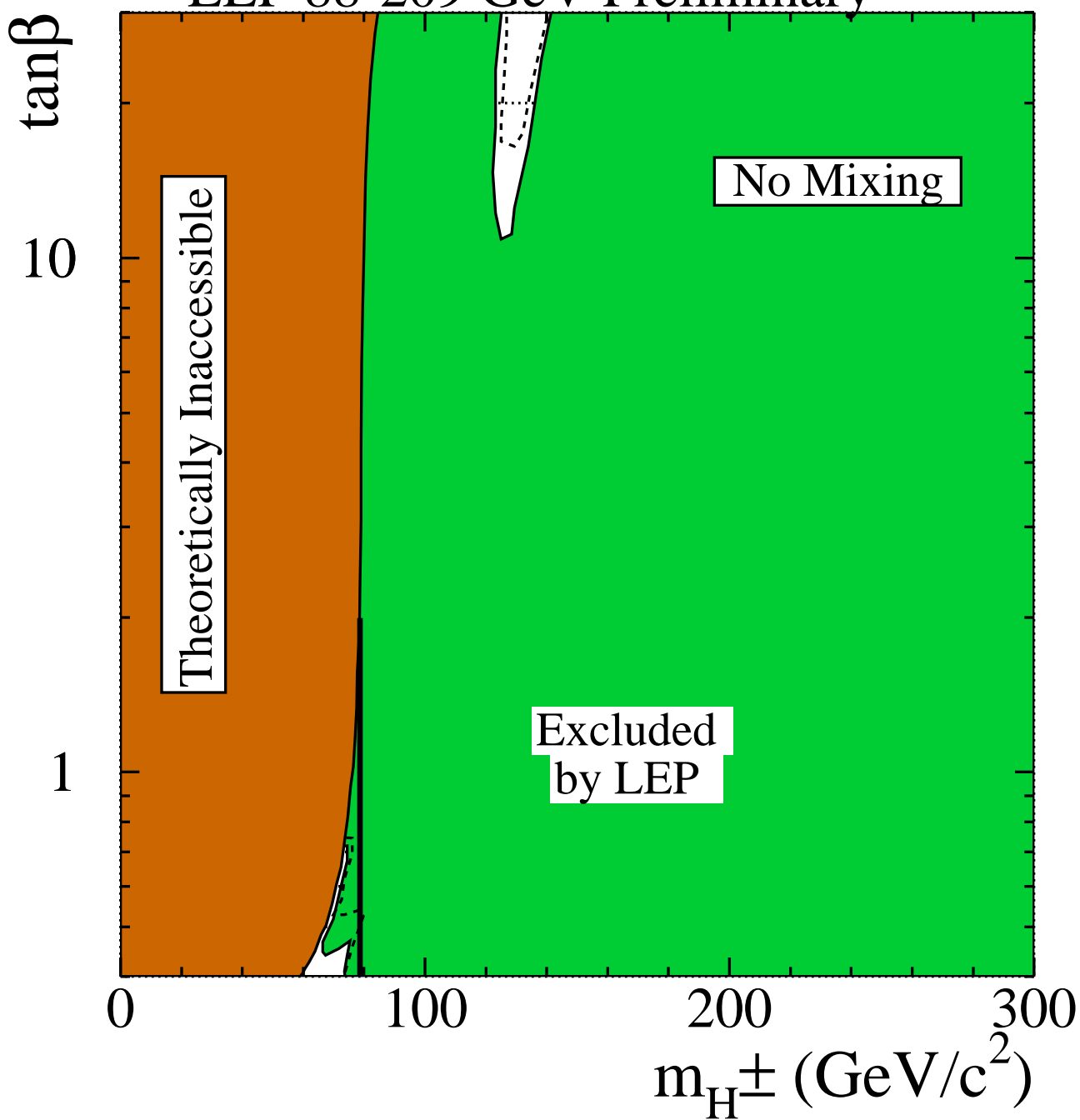


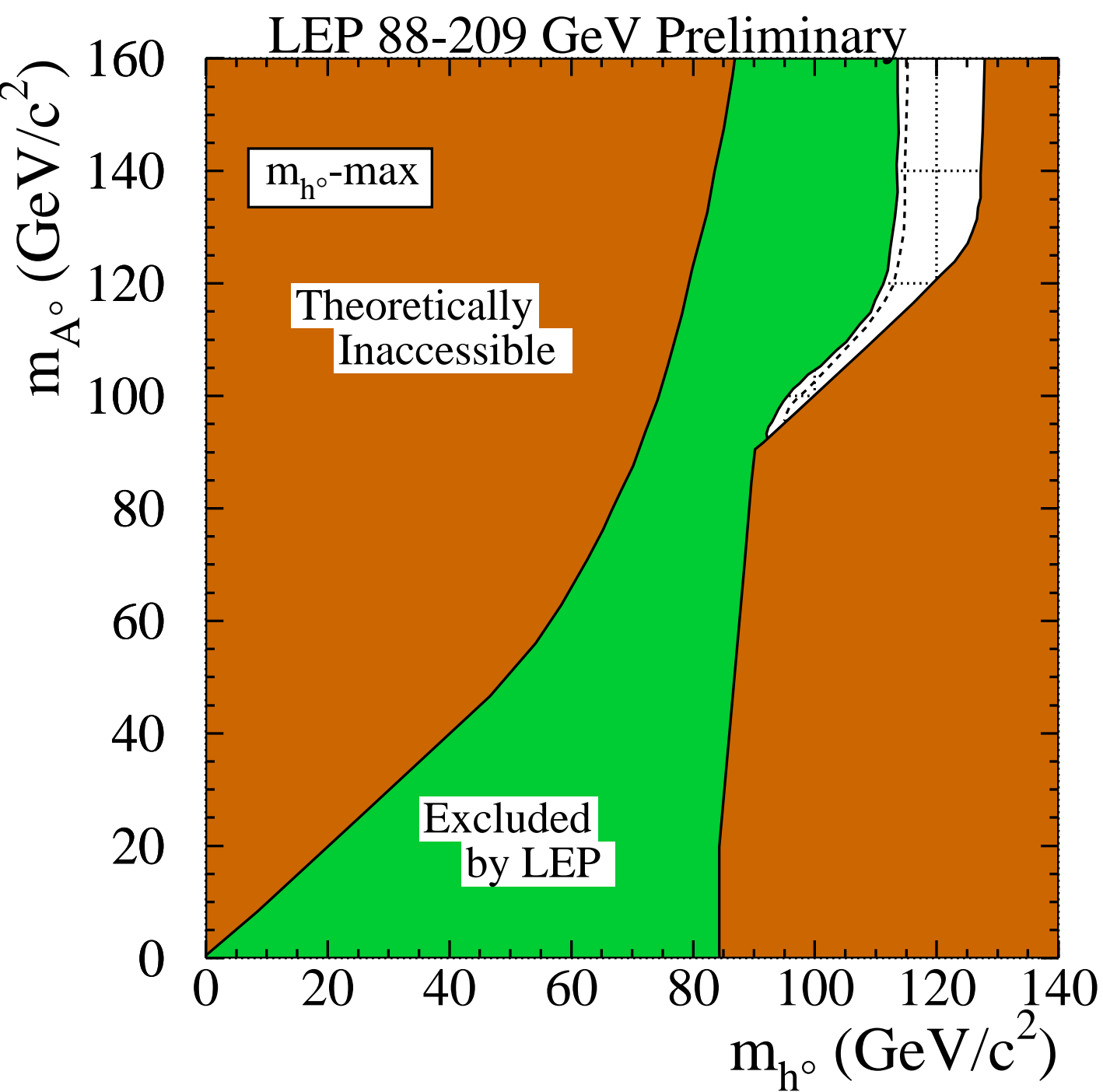
LEP 88-209 GeV Preliminary

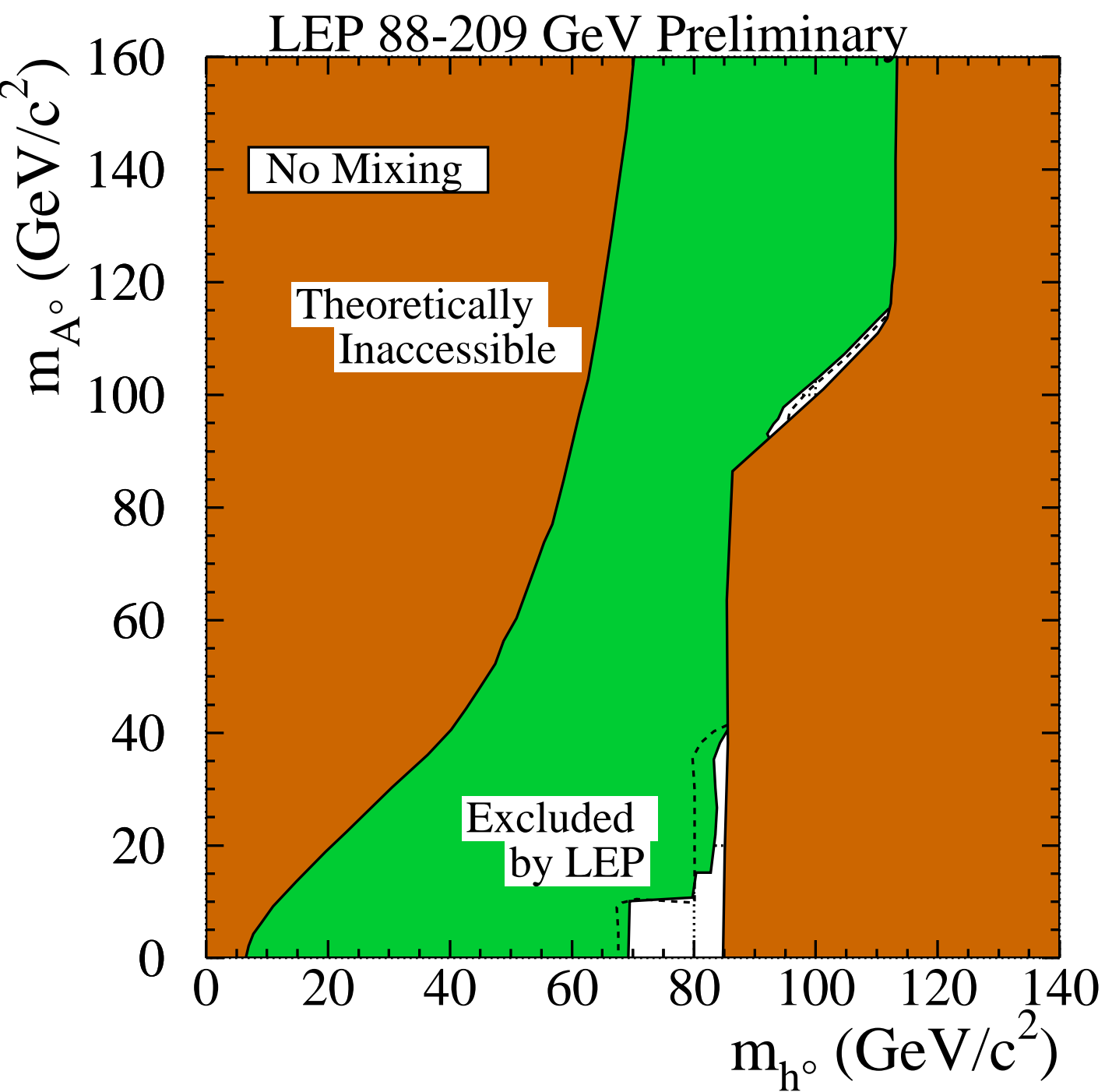




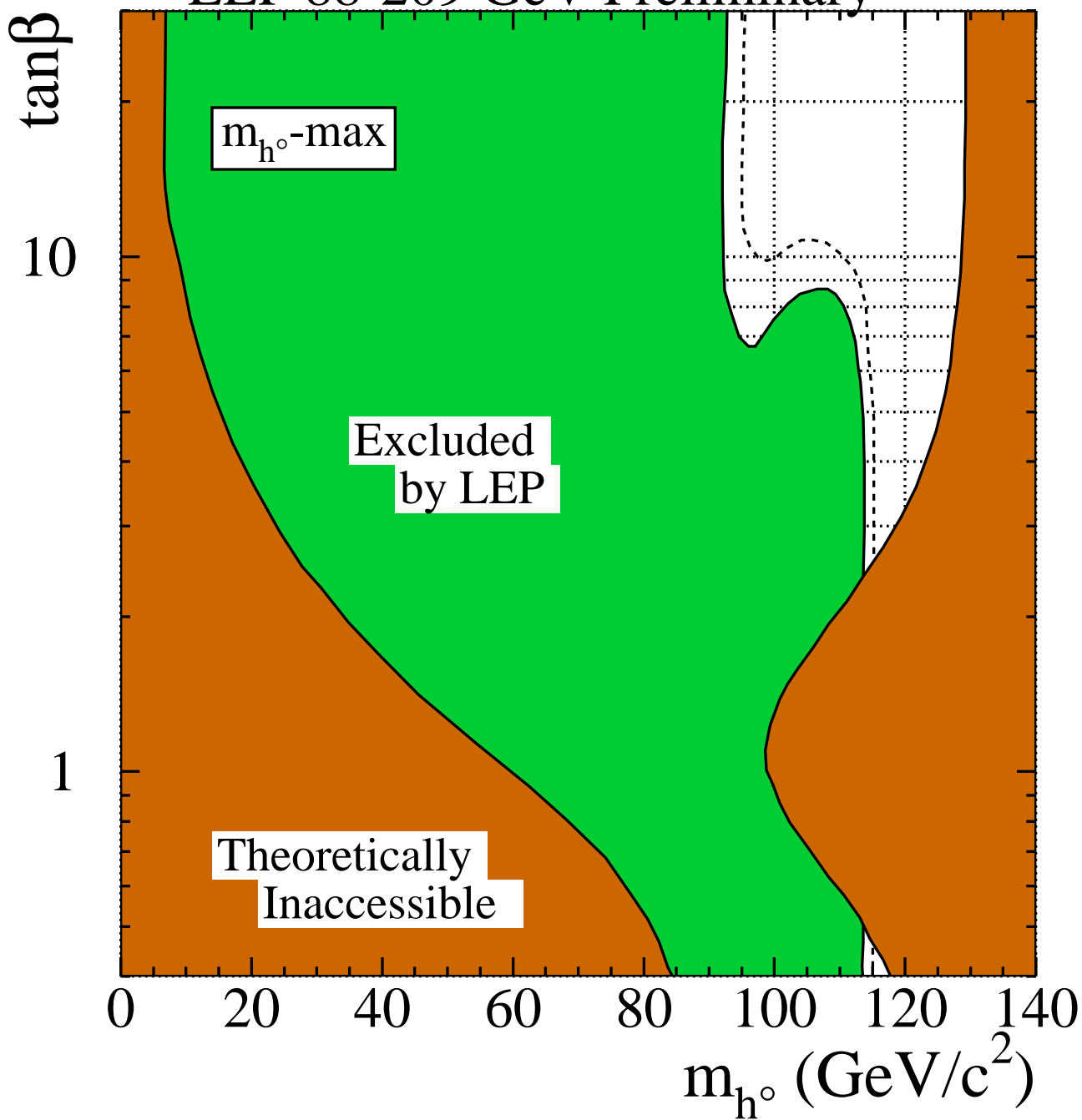
LEP 88-209 GeV Preliminary







LEP 88-209 GeV Preliminary



LEP 88-209 GeV Preliminary

